Shear thickening of cornstarch suspensions as a reentrant jamming transition

Fall, A.; Huang, N.; Bertrand, F.; Ovarlez, G.; Bonn, D.

DOI
10.1103/PhysRevLett.100.018301
Publication date
2008

Published in
Physical Review Letters

Shear Thickening of Cornstarch Suspensions as a Reentrant Jamming Transition

Abdoulaye Fall,[1,2] N. Huang,[1] F. Bertrand,[2] G. Ovarlez,[2] and Daniel Bonn[1,3]

[1]*Laboratoire de Physique Statistique de l'ENS, 24, rue Lhomond, 75231 Paris Cedex 05, France*

[2]*Laboratoire des Matériaux et Structures du Génie Civil, 2 Allée Kepler, 77420 Champs sur Marne, France*

[3]*Van der Waals–Zeeman Institute, University of Amsterdam, Valckenierstraat 65, 1018 XE Amsterdam, the Netherlands*

(Received 26 April 2007; published 8 January 2008)

We study the rheology of cornstarch suspensions, a non-Brownian particle system that exhibits shear thickening. From magnetic resonance imaging velocimetry and classical rheology it follows that as a function of the applied stress the suspension is first solid (yield stress), then liquid, and then solid again when it shear thickens. For the onset of thickening we find that the smaller the gap of the shear cell, the lower the shear rate at which thickening occurs. Shear thickening can then be interpreted as the consequence of dilatancy: the system under flow wants to dilate but instead undergoes a jamming transition because it is confined, as confirmed by measurement of the dilation of the suspension as a function of the shear rate.

DOI: 10.1103/PhysRevLett.100.018301 PACS numbers: 83.80.Hj

Complex fluids are immensely important in our everyday life (e.g., foodstuffs, cosmetics), for industry (concrete, crude oil), for understanding certain biological processes (blood flow), and so on. Such complex fluids are mostly suspensions of particles such as colloids, polymers, or proteins in a solvent. The majority of these suspensions exhibit shear thinning: the faster the material flows, the smaller its resistance to flow, or apparent viscosity [1]. For soft glassy materials, this is usually interpreted in terms of the free energy landscape of the system. If the system is sheared, the shear pulls the system over certain energy barriers that the system would not be able to cross without the applied shear; the viscosity consequently becomes small.

Because of the generality of the shear-thinning phenomenon, it is interesting to note that exceptions to the rule exist. Typically for certain concentrated suspensions of particles, shear thickening may be observed as an abrupt increase in the viscosity of the suspension at a certain shear rate [2]. The detailed mechanism of this shear-thickening phenomenon is still under debate [1–10]. For colloidal suspensions, the phenomenon is often attributed to the shear-induced formation of hydrodynamic clusters [3]: in this case, the viscosity increases continuously as a consequence of its dependence on particle configuration [4]; this may be but is not necessarily accompanied by an order-disorder transition in the particle configuration [5]. The viscosity rise can also be discontinuous at high volume fractions [5,6], probably because of aggregation of clusters creating a jammed network [7,8]. In the latter case, the clustered shear thickened state may be metastable [6,9].

In terms of the free energy landscape, this poses a challenging problem: why would some systems choose easy paths (shear thinning) while others opt for difficult ones (shear thickening)? One possible solution to this problem proposed recently [11] is that shear thickening is due to a reentrant jamming transition. It has been suggested for glassy systems that applying a shear is equivalent to increasing the effective temperature with which the system attempts to overcome energy barriers [12]. If now a system has a reentrant ''solid'' transition as a function of temperature, the ''solid'' phase may also be induced by the shear, leading to shear thickening [11].

In this Letter we study a well-known example of a shear-thickening suspension: cornstarch particles suspended in water [13]. We show that the shear thickening can in fact be viewed as a reentrant solid transition. The new findings are that (i) at rest the material is solid because it has a (small) yield stress; (ii) for low shear rate, shear banding (localization) occurs, and the flowing shear band grows with increasing shear rate, the shear thus liquefies the material; (iii) shear thickening happens at the end of the localization regime, where all of the material flows, subsequently it suddenly becomes ''solid'' again. In addition, (iv) we find a pronounced dependence of the critical shear rate for the onset of shear thickening on the gap of the measurement geometry, which can be explained by the tendency of the sheared system to dilate.

The cornstarch particles (Sigma) are relatively monodisperse particles with, however, irregular shapes [Fig. 4(b), inset]. Suspensions are prepared by mixing the cornstarch with a 55 wt % solution of CsCl in demineralized water. The CsCl allows one to perfectly match the solvent and particle densities [13]. We focus here on the behavior of a 41 wt % cornstarch suspension; all concentrated samples (between 30% and 45%) that we investigated showed a very similar behavior. Experiments are carried out with a vane-in-cup or plate-plate geometry on a commercial stress-controlled rheometer. The vane geometry is equivalent to a cylinder with a rough lateral surface which reduces wall slip [2]. The inside of the cup is also covered with the granular particles using double-sided adhesive tape. For the plate-plate geometry, the upper plate is of 40 mm diameter; both plates are roughened.

Velocity profiles in the flowing sample were obtained with a velocity controlled magnetic resonance imaging

(MRI) rheometer from which we directly get the local velocity distribution in a Couette geometry with a gap of 1.85 cm [14]. We investigated the stationary flows for inner cylinder rotational velocity Ω ranging between 0.2 and 10 rpm, corresponding to overall shear rates between 0.04 and 2.35 s^{-1}. The velocity profiles show that for low rotation rates of the inner cylinder, there is shear localization (Fig. 1): the velocity profile is composed of two regions: the part close to the inner cylinder is moving, and the rest is not. The MRI also allows us to measure the particle concentration; to within the experimental uncertainty of $\pm 0.2\%$ in volume fraction the particle concentration is homogeneous throughout the gap. This however does not completely rule out particle migration; we will estimate possible maximum migration below at around 0.1%. Thus, it is possible that the particle concentration in the flowing part of the material is slightly lower than that in the ''solid'' part.

Upon increasing the rotation rate, a larger part of the fluid is sheared, and for the highest rotation speeds the sheared region occupies the whole gap. We are unable to go to higher rotation rates since the shear thickening sets in when shear band occupies the whole gap of the Couette cell, and when it does the motor of the rheometer is no longer sufficiently strong to rotate the inner cylinder: shear thickening is observed as an abrupt increase of the measured torque on the rotation axis.

For the lower rotation speeds, since the part of the material that does not move is subjected to a stress, this means that the suspension has a yield stress. The yield stress can be determined from the critical radius r_c at which the flow stops: the shear stress at a given radius r as a function of the applied torque C and the fluid height H follows from momentum balance, and thus the yield stress at r_c follows immediately as $\tau_c = C/2\pi H r_c^2$. The yield stress turns out to be on the order of 0.3 Pa. Although it appears obvious that concentrated suspensions that show shear thickening also have a yield stress, we have not found literature comparing the prethickening flow behavior to a Herschel-Bulkley model as we do here. This is probably due to the fact that the yield stress is low: it is too small to be detected from a simple experiment such as an inclined plane test [15]. We can detect it relatively easily here because we use the MRI data. The stress for the MRI setup is measured on a rheometer with exactly the same measurement geometry as used in the MRI. In the flowing part, the shear rate can be deduced from the velocity profile $v(r)$ as $\dot{\gamma} = \frac{\partial v}{\partial r} - \frac{v}{r}$, where the second term on the right-hand side is due to the fact that in a Couette geometry the stress is not constant. Then, r can be eliminated from this equation when combined with the equation for the stress to deduce the constitutive equation of the fluid. This is shown in Fig. 1, and also shows that the suspension has a yield stress $\tau_c \approx 0.3$ Pa.

In the standard rheology experiments depicted in Fig. 2, the first important observation is that the critical stress for the onset of shear thickening is roughly constant at ≈ 20 Pa. This implies that there are two critical stresses for which the viscosity becomes infinite: First, upon approaching the yield stress from above, the viscosity diverges in a continuous fashion, in agreement with the MRI observations that the flow behavior is close to that of a Herschel-Bulkley fluid. Second, at the critical stress for thickening, a discontinuous jump of the viscosity is observed. When taken together, these results strongly resemble the theoretical proposition [11] that shear

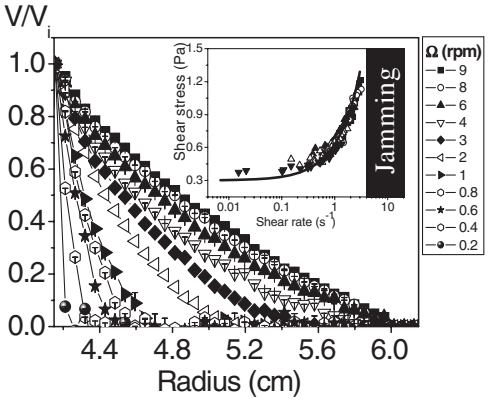

FIG. 1. Dimensionless velocity profile in the gap obtained by MRI measurements. Inset: Local shear stress as a function the local shear rate. The line is a fit to the Herschel-Bulkley model: $\tau = \tau_c + k\dot{\gamma}^n$ with $\tau_c = 0.3$ Pa, $k = 0.33$ Pa · s, and $n = 0.88$.

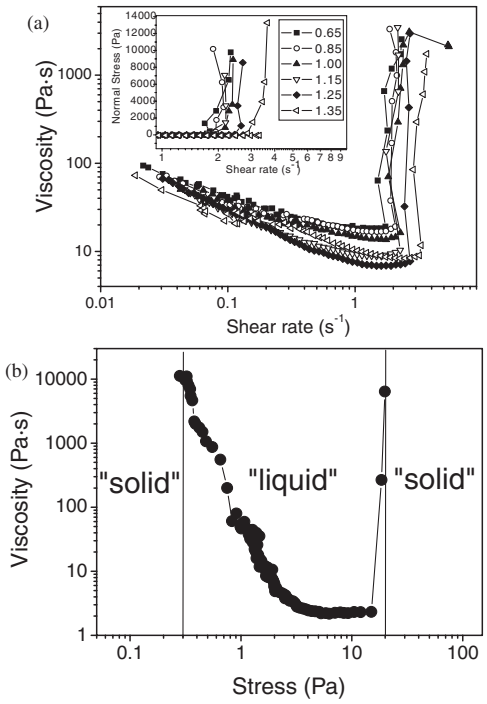

FIG. 2. (a) Apparent viscosity and normal stress as a function of shear rate for different gaps. Measurements were made with a plate-plate rheometer (Bohlin C-VOR 200) with radius $R = 20$ mm. (b) Viscosity as a function of applied stress, showing the reentrant jamming transition.

thickening is due to a reentrant jamming transition [Fig. 2(b)].

To pinpoint the mechanism of the thickening, a second important observation is that a significant difference in shear rate for the onset of shear thickening was observed between Couette cells with different gaps: 0.25, 1, and 3 mm gaps gave onset shear rates for shear thickening that systematically increased with increasing gap size, showing a linear increase of the critical shear rate on the gap. In order to investigate this in detail, we use a plate-plate cell so that we can vary the gap in a continuous fashion. This geometry has the additional advantage that there is no reservoir of particles present, as is the case at the bottom of the Couette cell, and in addition we can measure the normal stresses. The rheometer measures a torque C and a rotation rate ω, which are related to the stress and shear rate at the edge of the sample by $\tau = 3C/2\pi R^3$ and $\dot{\gamma} = 2\pi R\omega/b$, with R the plate radius and b the spacing. Figure 2 shows the measured apparent viscosity as a function of shear rate for different gaps. At a certain shear rate, a very abrupt increase in viscosity is observed; this critical shear rate increases with increasing gap. Comparison between plate-plate, cone-plate, and Couette cells showed identical critical shear rates to within the experimental uncertainty [16] showing that the shear rate gradient present in our plate-plate geometry does not strongly affect our results. We thus use the plate-plate cell only for the critical shear rate, which is well defined. For the quantitative determination of the constitutive law, on the other hand, we use the MRI data. No time dependence was observed, at least as long as the system had not thickened. Notably, we looked for time dependence in the viscoelastic properties, and the viscosity at a given imposed shear rate as a function of time for periods extending to days: no time evolution was observed.

Figure 2 also shows the normal stresses as a function of the shear rate. Again, an abrupt increase is observed at a shear rate that is very comparable to the shear rate found in the viscometry measurements. Defining the critical shear rate as the first shear rate for which the apparent viscosity goes up, or the lowest shear rate for which a measurable normal stress is observed, both are similar, and increase linearly with the gap between the plates.

A puzzling observation is that the results shown in Fig. 2 only hold when the surplus of paste around the plates is carefully removed. If a few milliliters of suspension is left on the bottom plate in contact with the paste between the two plates, the critical shear rate strongly increases and becomes independent of the gap size (Fig. 3).

The critical shear rate with a surplus is, in addition, the same as that found in the large-gap Couette cell, in which there is also a reservoir of particles present at the bottom of the inner cylinder. The flow curve of Fig. 1 shows that also in the MRI experiments exists a critical shear rate of about 4 s^{-1}; as soon as this shear rate is exceeded, the system shear thickens. We therefore conclude that in the classical rheology experiments the critical shear rate for thickening obeys $\dot{\gamma}_{c_M} = \dot{\gamma}_{c_I} - \alpha h$ for $h < h_c$ and constant above; here h is the gap, $\dot{\gamma}_{c_I} \approx 5.5\ s^{-1}$ is the critical shear rate that is intrinsic to the system $\dot{\gamma}_{c_M}$, and $\alpha = 0.22 \pm 0.04\ s^{-1}\,mm^{-1}$.

The principal information obtained from the normal stress measurement is their on-off behavior, which is quantitatively linked with the onset shear rate. The normal stresses are reminiscent of the Reynolds dilatancy of dry granular matter: when sheared, it will dilate in the normal direction of the velocity gradient. Dilatancy is a direct consequence of collisions between the grains: to accommodate the flow, the grains have to roll over each other in the gradient direction, and hence the material will tend to dilate in this direction. However, in our system, the grains are confined, both between the plates and in the solvent. The latter provides a confining pressure that is mainly due to the surface tension of the solvent, making it impossible to remove grains from the suspension. As suggested by Cates *et al.* [17], the confinement pressure associated with this should be on the order of the surface tension over the grain size, $P_c = \gamma/R \approx 7000$ Pa, of the same order of magnitude as the typical normal stresses measured in the experiments near the onset of shear thickening. In addition, this gives a maximal dilation that is on the order of 1 particle diameter ($\approx 20\ \mu$m); compared to the radius of the plate-plate cell this gives a maximum dilation of about 0.1%, too small to be detected by our MRI density measurements.

It is tempting to see whether the shear-thickening phenomenon itself can be due to the confinement: if the cornstarch is confined in such a way that the grains cannot roll over each other, this could in principle lead to an abrupt jamming of the system. In our rheometer, instead of setting the gap size for a given experiment, we can impose the normal stress and make the gap size vary in order to reach the desired value of the normal stress. If this is done for different shear rates, and the target value for the normal stress is taken to be zero, we can obtain the dependence of the gap variation on shear rate $d\Delta h/d\dot{\gamma}$. A typical measurement is shown in Fig. 4(a), where we impose a constant

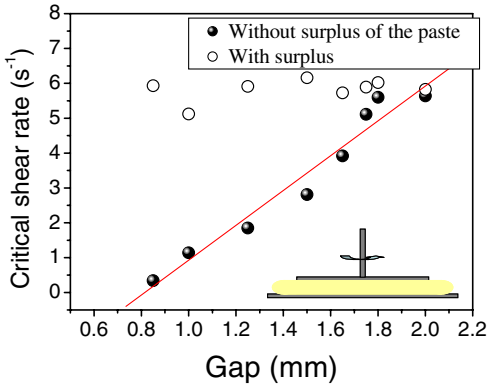

FIG. 3 (color online). Evolution of the critical shear rate a function of the gap.

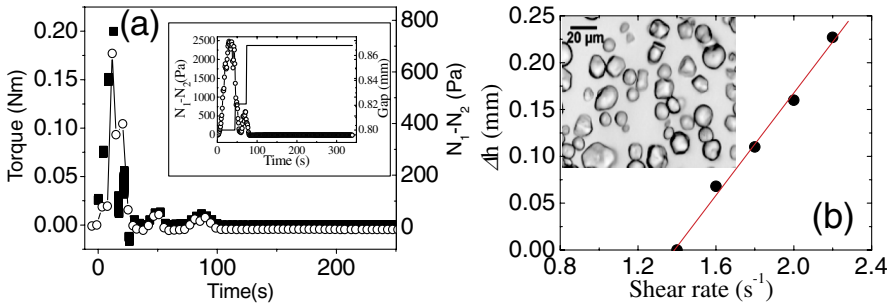

FIG. 4 (color online). (a) Time evolution of the torque and the normal stress for $\dot{\gamma} = 1.6\ \mathrm{s}^{-1}$. Inset: Evolution of the normal stress and the gap. Torque (squares), N_1-N_2 (circles), gap (line). (b) Variation of the gap according to the shear rate. Inset: Micrograph of the cornstarch particles.

shear rate and measure the gap and viscosity as a function of time. This shear rate and initial gap combination are beyond the shear-thickening transition in shear rate, and thus the viscosity starts to strongly increase, as do the normal stresses. The latter leads to an increase in the gap, allowing the system to dilate, until the shear thickening disappears altogether: the viscosity is back to low values. This unambiguously demonstrates that the shear thickening is a dilation effect, and that taking away a confining factor makes the thickening disappear altogether. Measurements comparing plate-plate and cone-plate show very similar behavior; this suggests that by far the dominant contribution to the normal stress difference in the plate-plate cell comes from N_1. Dilation measurements with and without a surplus of paste show very similar behavior (although of course at slightly different shear rates). This shows that it is indeed the normal stress differences rather than the normal stresses that are important.

More quantitatively, repeating this experiment for different shear rates [Fig. 4(b)], one can obtain the gap change as a function of the shear rate that allows the suspension to flow freely, i.e., without developing normal stresses due to particle collisions. The linear evolution of Δh with the shear rate $\Delta h = \alpha^{-1}\dot{\gamma}_c$ with $\alpha = 0.27 \pm 0.03\ \mathrm{s}^{-1}\,\mathrm{mm}^{-1}$ is completely consistent with the α value of Fig. 3, providing a quantitative check that indeed the dilatancy is responsible for the shear thickening. It also explains why leaving paste around the measurement geometry increases the critical shear rate: the extra suspension acts as a reservoir, in which the sheared suspension can dilate.

In conclusion, the effect of shearing is to first unjam a jammed (yield stress) system, and for higher stresses jam the unjammed system because of the confinement. This leads to a solid-liquid-solid transition as a function of the applied stress. In terms of the free energy landscape picture of sheared glassy systems, our results show that it is not sufficient to consider just the shear stresses in determining how an imposed flow affects the relaxation time or viscosity of the system: the normal stress differences that arise from the flow itself have to be considered also. Thus, the exception to the rule that all complex fluids are shear thinning is likely to be due to other components of the stress tensor, which have not been considered in the explanation of shear thinning in terms of the free energy landscape [12].

[1] R. G. Larson, *The Structure and Rheology of Complex Fluids* (Oxford, New York, 1999).
[2] H. A. Barnes, J. Rheol. (N.Y.) **33**, 329 (1989); A. A. Catherall, J. R. Melrose, and R. C. Ball , J. Rheol. (N.Y.) **44**, 1 (2000).
[3] J. W. Bender and N. J. Wagner, J. Colloid Interface Sci. **172**, 171 (1995); J. Rheol. (N.Y.) **40**, 899 (1996); B. J. Maranzano and N. J. Wagner, J. Chem. Phys. **117**, 10 291 (2002); J. Rheol. (N.Y.) **45**, 1205 (2001); D. R. Foss and J. F. Brady, J. Fluid Mech. **407**, 167 (2000).
[4] G. Marrucci and M. M. Denn, Rheol. Acta **24**, 317 (1985).
[5] R. L. Hoffman, J. Rheol. (N.Y.) **42**, 111 (1998); Trans. Soc. Rheol. **16**, 155 (1972); J. Colloid Interface Sci. **46**, 491 (1974).
[6] E. Bertrand, J. Bibette, and V. Schmitt, Phys. Rev. E **66**, 060401 (2002); D. Lootens *et al.*, Phys. Rev. Lett. **90**, 178301 (2003); **95**, 268302 (2005).
[7] J. R. Melrose and R. C. Ball, Europhys. Lett. **32**, 535 (1995); R. S. Farr, J. R. Melrose, and R. C. Ball, Phys. Rev. E **55**, 7203 (1997).
[8] M. E. Cates *et al.*, Phys. Rev. Lett. **81**, 1841 (1998).
[9] R. J. Butera *et al.*, Phys. Rev. Lett. **77**, 2117 (1996).
[10] G. Bossis and J. F. Brady, J. Chem. Phys. **91**, 1866 (1989); J. R. Melrose and R. C. Ball, J. Rheol. (N.Y.) **48**, 937 (2004).
[11] C. B. Holmes, M. Fuchs, and M. E. Cates, Europhys. Lett. **63**, 240 (2003); C. B. Holmes *et al.*, J. Rheol. (N.Y.) **49**, 237 (2005); M. Sellito and J. Kurchan, Phys. Rev. Lett. **95**, 236001 (2005).
[12] L. Berthier, J.-L. Barrat, and J. Kurchan, Phys. Rev. E **61**, 5464 (2000).
[13] F. S. Merkt *et al.*, Phys. Rev. Lett. **92**, 184501 (2004).
[14] G. Ovarlez, F. Bertrand, and S. Rodts, J. Rheol. (N.Y.) **50**, 259 (2006).
[15] P. Coussot, Q. D. Nguyen, H. T. Huynh, and D. Bonn, J. Rheol. (N.Y.) **46**, 573 (2002).
[16] See EPAPS Document No. E-PRLTAO-100-015801 for a supplementary figure. For more information on EPAPS, see http://www.aip.org/pubservs/epaps.html.
[17] M. E. Cates, M. D. Haw, and C. B. Holmes, J. Phys. Condens. Matter **17**, S2517 (2005).